Chapter 2

Active polar flock with birth and death

2.1 Introduction

In chapter 1, we introduced the historical context and description of active systems. In this chapter, I will discuss the phase transition in the collective behaviour of polar flocks with birth and death. The phenomenon of collective behavior is being studied with great interest in systems exhibiting nonequilibrium phase transition under driven noise and particle density [Bhattacherjee et al. (2015); Buttinoni et al. (2013); Chaté et al. (2008); Pattanayak & Mishra (2018b); Singh et al. (2021c); Toner & Tu (1995)]. In different experimental [Deseigne et al. (2010); Narayan et al. (2007); Sahu & Dhara (2021); Sprenger et al. (2020); Zheng et al. (2013)], analytical [Di Carlo & Scandolo (2022); Toner & Tu (1995, 1998b); Toner et al. (2005b)] and numerical [Bhattacherjee et al. (2015); Cavaiola & Mazzino (2021); Daddi-Moussa-Ider et al. (2020); Das et al. (2018a); Delhaye et al. (2021); Dhar et al. (2021); Dwivedi et al. (2021b); Kumar & Mishra (2020a); Lian & Zhong (2021); Malvar & Cunha (2021); Nagilla et al. (2018); Pattanayak & Mishra (2018b); Sahoo et al. (2021); Singh et al. (2021c, 2022); Vinze et al. (2021)] studies of active matter systems it has been shown that the system changes its static and dynamic behaviour in different homogeneous and inhomogeneous environments and on the variation of different parameters [Deußen et al. (2022); Dhar et al. (2020); Dikshit & Mishra (2022); Durve & Sayeed (2016); Dwivedi et al. (2021a); Dyer & Ball (2021); Giomi et al. (2010); Kumar et al. (2021a); Marchetti et al. (2013b); Ramaswamy et al. (2003); Rank & Voigt (2021); Semwal et al. (2021); Singh & Mishra (2020)]. Similar to the phase behavior observed in conserved and non-conserved spin models [Puri (2009)], the flocking transition also exhibits different characteristics depending on whether the system's total particle number (analogous to

magnetization in spin models) is conserved or not. The nature of phase transition is one of the most studied phenomenon in this field [Bhattacherjee et al. (2015); Chaté et al. (2008); Durve & Sayeed (2016); Pattanayak & Mishra (2018b); Peruani et al. (2011); Singh et al. (2021c); Solon & Tailleur (2013, 2015)]. The phase transition in the collection of self-propelled particles also called as “flocking transition” is important, because it can be described as a nonequilibrium analog of disorder-to-order phase transition in equilibrium systems [Peruani et al. (2011); Solon & Tailleur (2013, 2015); Vicsek et al. (1995)].
In recent study of lattice based models introduced by Peruani *et al.* [Peruani et al. (2011)] and Solon *et al.* [Solon & Tailleur (2013)], it has been found that the nature of phase transition in self-propelling agents is analogous to the liquid-gas transition on the variation of temperature and density in the system [Solon & Tailleur (2013, 2015)]. To understand the phase transition Solon *et al.*] introduced a microscopic lattice model with discrete symmetry, which is known as active Ising model (AIM) [Solon & Tailleur (2013)]. The AIM is much simplified model for the collective motion and gives the basic features of the flocking models [Solon & Tailleur (2015)]: viz, band formation, large density fluctuations, discontinuous disorder-to-order phase transition etc. The study of AIM by [Solon & Tailleur (2013)] is for the system where total number of agents is fixed. The effect of birth and death [Toner (2012)] of agents on the nature of phase transition is not yet explored.
In this current study we ask the question: whether the introduction of birth and death of the agents can affect the nature of phase transition? To serve this purpose, we introduced a minimal lattice based-model of active Ising spins (AIM) with an additional birth and death term γ.
The system is studied for various γ and it is found that for the $\gamma = 0$, the system shows a first order, disorder-to-order phase transition with the appearance of bands in the local density and magnetisation. On introducing γ, the bands start to dilute and finally disappear for large γ and transition becomes continuous in nature. We also studied the system using coarse-grained hydrodynamic equations of motion. Using renormalised mean field theory we write an effective free energy for local order parameter and find an additional cubic order nonlinearity present for zero birth and death and the nonlinearity weakens on increasing birth and death parameter.

2.2 Model and Numerical Methodology

We consider a system of active Ising spins (AIM) on a two-dimensional rectangular lattice of size $L_x \times L_y$ with periodic boundary condition in both directions. A fraction of sites

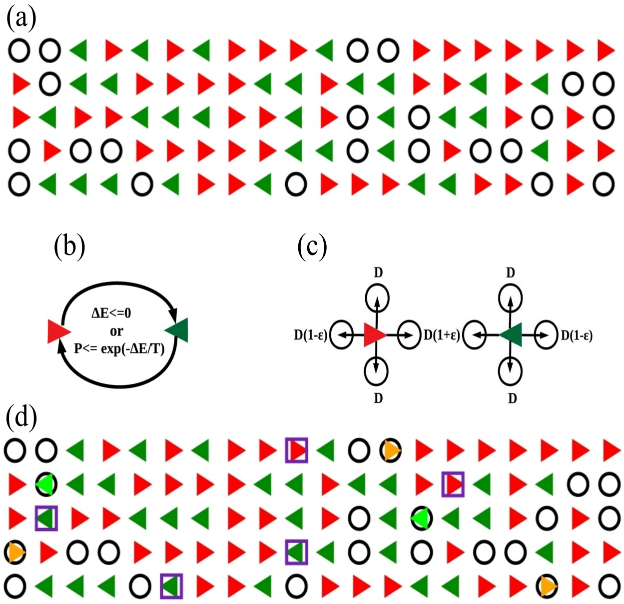

Fig. 2.1 **(a)** Sketch of a part of system carrying spins $S = +1$(red (triangle right)) and $S = -1$(dark green (triangle left)) along with vacant sites S=0(black circle) on a two-dimensional lattice, **(b)** represents the flipping rate at fixed temperature, **(c)** represents the probability of movement of the spins to the neighboring sites and in **(d)** the birth and death parameter γ is added in the model in which the particles disappearing from random sites is shown by magenta square and appearing at the sites which were vacant represented by orange triangle right for $S = +1$ and green triangle left for $S = -1$.

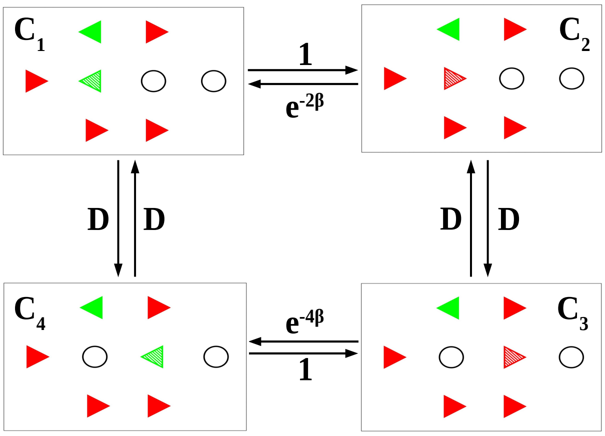

Fig. 2.2 A loop of four configurations that breaks Kolmogorov's criterion [Kolmogorov (1936)] of detailed balance for dIm, flipping and movement is shown for the spin represented by partially filled (red (triangle right)) and (dark green (triangle left)). The clockwise loop $(C_1 \to C_2 \to C_3 \to C_4 \to C_1)$ gives the total probability $D^2e^{-4\beta}$ while the anticlockwise loop $(C_1 \to C_4 \to C_3 \to C_2 \to C_1)$ gives the total probability $D^2e^{-2\beta}$, thus showing that the system does not satisfy detailed balance. The numbers associated to the arrows are the transition rates and other symbols have the same meaning as in Fig.[2.1].

on the lattice is vacant. Each spin can take two possible values $S_i = \pm 1$. Since some of the sites are vacant, we define an occupancy variable $n_i = 0$ or 1 for the unoccupied and occupied sites respectively. In this model, volume exclusion principle is effective such that each site can have maximum one particle on it [Mishra & Mishra (2023); Peruani et al. (2011)]. Each spin can interact with its nearest neighbor spins using the Ising Hamiltonian [Ising (1925)]

$$H = -\sum_{i=1}^{N} n_i n_j S_i S_j, \tag{2.1}$$

thus the interaction term is non-zero only if the site and the interacting sites both are occupied. The above Hamiltonian in Eq.(2.1) is simulated for a fixed vacancy density $V = 20\%$ (particle density $\rho = 0.8$) by tuning the temperature. The temperature is introduced through the Metropolis Monte-Carlo algorithm [Landau & Binder (2005); Pathria & Beale (2011)] for the alignment interaction among the spins. The ratio of the interaction strength and the Boltzmann constant is chosen as 1. Particles tend to move in the direction of their spin if the lattice site is vacant, otherwise, they do not move. The dynamics of the spins on the lattice can be modeled in the following manner: (i) the spins are fixed to their lattice sites and interacts through the Hamiltonian in Eq.(2.1). In this study, we are defining it as "fixed Ising model" (fIm). (ii) We allowed the spin to diffuse to any of its nearest

vacant site with equal probability. The model is named as diffusive Ising model (dIm). In Fig.[2.2] we show the Kolmogorov diagram [Kolmogorov (1936)] to check the detail balance condition on dIm. In Fig.[2.2], a loop of four configurations is shown, that breaks Kolmogorov's criterion, e.g. clockwise loop gives the total probability $D^2e^{-4\beta}$ while anticlockwise loop gives $D^2e^{-2\beta}$, thus showing that the system does not satisfy detailed balance. The numbers associated to the arrows are the transition rates. Hence fIm satisfies the detail balance condition but the dIm deviates from it and this observation is consistent with the model studied in [Peruani et al. (2011)].
(iii) Further we made the spins active by introducing a biased movement corresponding to their direction as introduced in [Solon & Tailleur (2013, 2015)]. The update rules showing the motion of the spins is shown in Fig.[2.1](b). Activity is introduced through a parameter $\varepsilon \in (0,1)$. In the presence of activity ε, the update rule for the movement of the spins at a particular site is given as follows. Each particle hops to its two neighboring sites left and right at rate $D(1+S\varepsilon)$ provided the target site is vacant. It hops to other two sites (up and down) with equal probability D. If the $\varepsilon = 0$, then the hoping rates are same in all the directions and that rate comes out to be $D = 1/4$ and the model reduces to dIm. For nonzero ε, the particle moves in the direction of its orientation at rate $D(1+\varepsilon)$ and in the opposite direction to its orientation at rate $D(1-\varepsilon)$. Whereas the particle hops with rate D to other two possible directions. For our present study we fix $\varepsilon = 1.0$. We call the model as active model (Am).
(iv) Next we introduce the birth and death of particles in the model (Am). The birth and death rate γ is introduced as a fraction of sites on the lattice with particle density ρ, such that from the randomly chosen $\gamma/2$ fraction of sites we remove the particles (if occupied) and similarly on the randomly chosen unoccupied sites i.e. $\gamma/2$ fraction of total number of sites, we introduced the new particles with spin favoured with the majority spins in their nearest neighbor. We call it birth and death active model $(bdAm)$, the value of γ is tuned from 0 to 0.1. For $\gamma = 0$, model reduces to Am. One simulation step is counted after successful update of the above steps for all the particles once. Total simulation steps (time) used is $T = 1.7 \times 10^5$. The steady state calculation of various quantities is performed after simulation time 7×10^4.We use 15 independent realizations for averaging the data for the system sizes $L_x \times L_y = 400 \times 50$, 600×50 and 800×50.

2.3 Results

We first studied the model $(bdAm)$ with no birth and death rate i.e. $\gamma = 0$. The system is studied by varying temperature. A disorder-to-order phase transition is found on decreasing

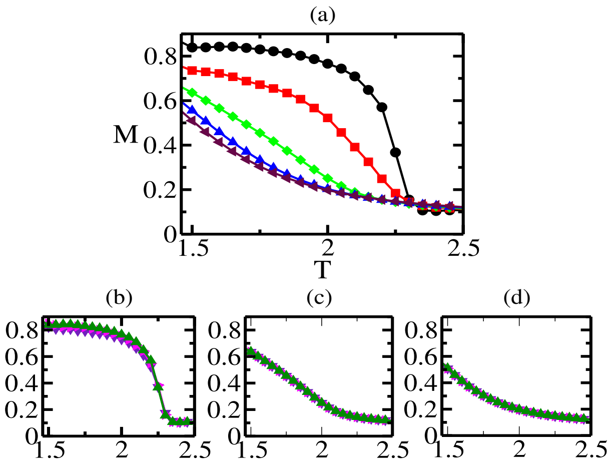

Fig. 2.3 The plot of order parameter M vs. temperature T (a) for the system size 800×50 and various values of γ i.e. The black (circle), red (square), green (diamond), blue (triangle right) and maroon (triangle left) for $\gamma = 0$, $\gamma = 0.01$, $\gamma = 0.1$, $\gamma = 0.5$ and $\gamma = 1$ respectively. The panels (b), (c) and (d) represent M vs. T for fixed $\gamma = 0$, $\gamma = 0.1$ and $\gamma = 1$ respectively. The different curves in each panel (b)-(d) represent different system sizes i.e. the indigo (triangle down), magenta (triangle right) and green4 (triangle right) for $400 \times 50, 600 \times 50$ and 800×50. The lines are guide to the eyes.

temperature. We studied the system for activity $\varepsilon = 1$ and for different γ. We first calculated the global magnetisation in the system defined as:

$$M(t) = \frac{1}{N} \mid \sum_i S_i(t) \mid \tag{2.2}$$

where N is total number of particles. We define the mean magnetisation $M =< M(t) >$, where $< .. >$ means the average over time in the steady state and over different realisations. We find that for the high temperature and for all γ, the system is disordered ($M \simeq 0$), and ordered with $M \simeq 1$ for low temperature.

The variation of M as a function temperature is shown in Fig.[2.3](a) for different γ. We find a very strong dependence of the shape of the disorder-to-order curve on γ. Also, we show the variation of M as a function of temperature for different system sizes $L_x \times L_y = 400 \times 50$, 600×50 and 800×50 for fixed value of $\gamma = 0.0$, 0.1 and 1.0 in Fig.[2.3] (b)-(d) respectively. We observe a very insignificant change in the curves with respect to system size and we expect that the present model has very weak finite size effect in comparison to other studies of Vicsek's type models [Chaté et al. (2008)].

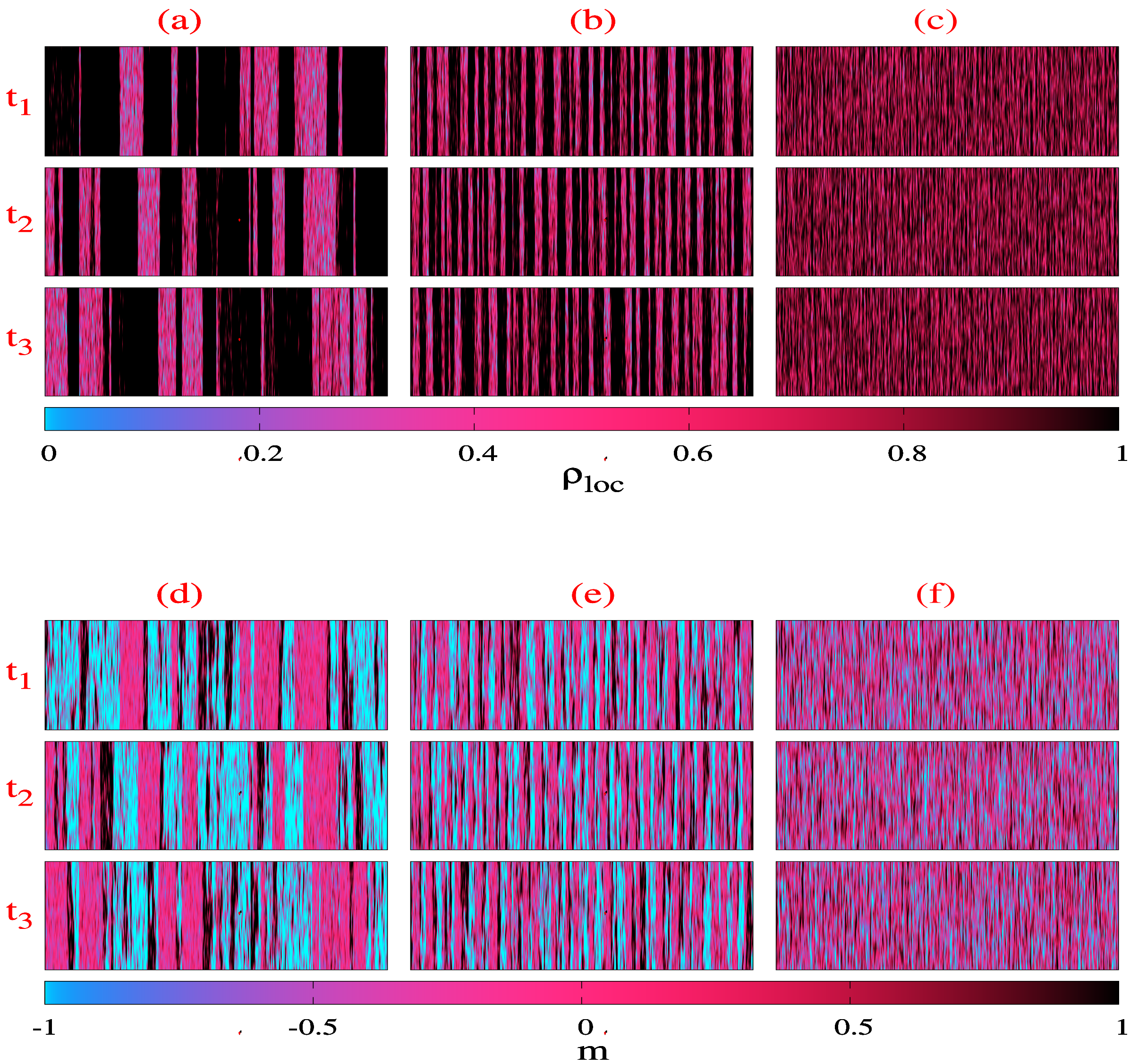

Fig. 2.4 Time snapshots of local density ρ_{loc} (a-c) and local magnetisation m (d-f). From left to right (a-c) or (d-f) is for $\gamma = 0.0$, 0.01 and 0.1 and (t_1-t_3) is for 1.4×10^5, 1.5×10^5, 1.6×10^5 respectively. Color bars represent the value of local density ρ_{loc} and magnetisation m. System size is 400×50 and only a part of the system is shown for better resolution.

To confirm the nature of transition, we looked the system near to the disorder-to-order transition. We first plot the real space snapshot of local density ρ_{loc} in Fig.[2.4](a-c). The ρ_{loc} is calculated by counting the density of spins in box of size 2×2. The panels from top to bottom (t_1 - t_3) for three different simulation times $t = 1.4 \times 10^5$, 1.5×10^5 and 1.6×10^5 respectively. The panel (a)-(c) is for $\gamma = 0$, 0.01 and 0.1 respectively. For $\gamma = 0$, we see the formation of bands of high density spins and with the time these bands move across the system. The bands get diluted on increasing γ and disappear for large value $\gamma = 0.1$. The color bar shows the value of local density ρ_{loc}. Similarly we also plot the local magnetisation m, obtained by calculating the mean spin in the box of size 2×2 in Fig.[2.4](d-f) for the same set of parameters as for (a-c). The panel (d-f) is for $\gamma = 0$, 0.01 and 0.1 respectively. We again find for zero γ, bands of high ordered region moves in the background of disordered region. The bands get diluted on increasing γ and finally disappear for large $\gamma = 0.1$. The color bar shows the value of local m and positive and negative m represents the mean local spin $+1$ and -1 respectively. Very clearly the band splits into thinner and weaker bands on the introduction of γ. The formation of bands we find here for $\gamma = 0$ or Am is a common characteristics of polar flock [Chaté et al. (2008); Mishra et al. (2010); Peruani et al. (2011); Solon & Tailleur (2013, 2015)]. For large $\gamma \simeq 0.1$ slowly the density pattern disappears and its all become close to mean density $\rho_{loc} = 0.8$.

To further characterise the density inhomogeneity for different γ we plot the distribution of density for different temperatures close to disorder-to-order transition. Using the the local density ρ_{loc} plots shown in Fig.[2.4](a-c), we calculated the local density along the long axis of the system by averaging over the shorter axis L_y. In this manner we find the density variation in one direction ρ_x. We further plot the probability distribution function (PDF) of density $P(\rho_x)$ for various γ in Fig.[2.5]. For zero γ, distribution clearly shows the bimodal nature, with one peak close to 1 (maximum density) and another peak at lower density $\rho_x = 0.4$. As we increase γ the two peaks come closer and finally for $\gamma \geq 0.1$ we find a single peak at $\rho_x = 0.8$. In inset of Fig.[2.5] we plot the density difference of two peaks $\Delta\rho$ vs. γ, and plot clearly shows a monotonic decrease of $\Delta\rho$ on increasing γ.
To understand the effect of γ on the nature of phase transition in the system we observed time series of the global magnetisation $M(t)$ in the steady state for two different $\gamma = 0$ and $\gamma = 0.1$. Using the time series we calculated the probability distribution function (PDF) of magnetisation $P(M)$. In Fig.[2.6] we plot the $P(M)$ in the vicinity of disorder-to-order transition. Fig.[2.6](a) and (b) show the $P(M)$ for $\gamma = 0$ and $\gamma = 0.1$ respectively. Fig.[2.6](a), shows a bimodal distribution of $P(M)$ with one peak at $M = 0.05$ and another

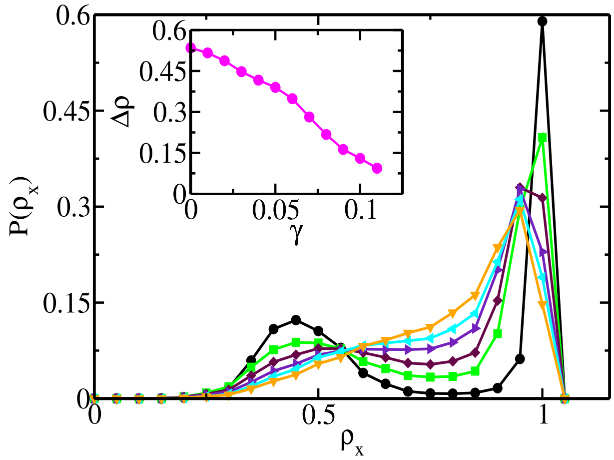

Fig. 2.5 Plot of PDF $P(\rho_x)$ for different values of γ i.e. The black (circle), green (square), maroon (diamond), indigo (triangle right), cyan (triangle left) and orange (triangle down) symbols represent $\gamma = 0$, $\gamma = 0.02$, $\gamma = 0.04$, $\gamma = 0.06$, $\gamma = 0.08$ and $\gamma = 0.1$ respectively. The lines are guide to eyes. Inset: plot of $\Delta\rho$ vs. γ where $\Delta\rho$ represents the difference between two peaks of the distribution of local density. The system size is same as in Fig.[2.4

].

at $M = 0.45$ for some intermediate temperature $T = 2.25$ and in the neighborhood of $T = 2.25$, $T = 2.15, 2.20, 2.30, 2.35$ we find jump in the peak position of $P(M)$. Whereas the distribution is always unimodal for all T and the location of peak in $P(M)$ smoothly moves towards lower M values for $\gamma = 0.1$ as shown in Fig.[2.6](b). Hence we say that the nature of the phase transition changes from the discontinuous to continuous type on increasing γ. In this paper, we mainly focused on the effect of birth and death (*bdAm*). We also performed study for zero birth and death and varying the activity $\varepsilon \in (0, 1)$. We found that the nature of phase transition and the behaviour of magnetisation vs. temperature curves changes from continuous to discontinuous type on varying ε (data not shown). These findings are consistent with the study of Peruani *et al.* [Peruani et al. (2011)].
Now using coarse-grained hydrodynamic equations of motion we show how the increasing birth and death parameter in the density equation can lead to continuous transition.

2.4 Hydrodynamic equations of motion for slow variables

Now we introduce the coarse-grained hydrodynamic equations of motion for slow variables: density $\rho(\mathbf{r}, t)$ and polarisation order parameter $\mathbf{P}(\mathbf{r}, t)$. Former is globally conserved and later is nonzero for the broken symmetry or ordered state. The equation of motion for local

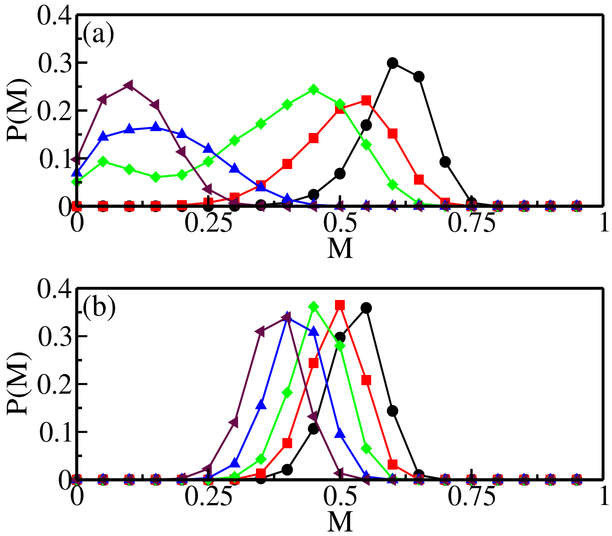

Fig. 2.6 Plot of PDF of order parameter $P(M)$ for $\gamma = 0$ and $\gamma = 0.1$ in (a) and (b) respectively, where the black (circle), red (square), green (diamond), blue (triangle left) and maroon (triangle up) symbols represents the temperatures (a) $T = 2.15$, $T = 2.20$, $T = 2.25$, $T = 2.30$ and $T = 2.35$ respectively and (b) $T = 1.65$, $T = 1.70$, $T = 1.75$ $T = 1.80$ and $T = 1.85$ respectively near the disorder-to-order transition. Lines are guide to eyes. The system size is same as in Fig.[2.4]

.

density field $\rho(\mathbf{r},t)$

$$\frac{\partial \rho}{\partial t} = -v_0 \nabla.(\mathbf{P}\rho) + D_\rho \nabla^2 \rho + \gamma g(\rho) \tag{2.3}$$

and the hydrodynamic equation of motion for the local polarisation $\mathbf{P}(\mathbf{r},t)$,

$$\frac{\partial \mathbf{P}}{\partial t} = (\alpha_1(\rho) - \alpha_2 \mid \mathbf{P} \mid^2)\mathbf{P} - v_1 \nabla \rho + \lambda(\mathbf{P} \cdot \nabla \mathbf{P}) + D\nabla^2 \mathbf{P} \tag{2.4}$$

Eq.(2.3) represents continuity equation with additional birth and death term $g(\rho) = \rho(\rho_0 - \rho)$ for the density field ρ. Where ρ_0 is the mean density of particles in the system and γ is the birth and death parameter. This type of term was first put by Malthus [Malthus (1798)] and consequently the flocks with birth and death are also known as Malthusian flocks. According to Malthus, any collection of entities that is reproducing and dying can only reach a non-zero steady state with population density ρ_0. $g(\rho)$ increases with increasing ρ for $\rho < \rho_0$ and it decreases with increasing ρ for $\rho > \rho_0$. The first term on the right hand side of Eq.(2.3), describes the convection due to self-propulsion velocity $v_0\mathbf{P}$. The second term on the right hand side of Eq.(2.3) is diffusion due to density gradient. In polarisation $\mathbf{P}(\mathbf{r},t)$, Eq.(2.4), the first term on right hand side represents a mean field transition from an isotropic state ($\mathbf{P} = 0$) to a broken symmetry state $\mathbf{P} = \sqrt{\frac{\alpha_1(\rho_0)}{\alpha_2}}\hat{\mathbf{x}}$ (the direction of broken symmetry is chosen the along $x-$axis). The second and third term indicate hydrostatic pressure due to density gradient and convection in the model, respectively. Both λ and v_1 depends on self-propelled speed of the particle [Bertin et al. (2006a)]. The fourth term represents diffusion in the polarisation field. The above two equations are similar to the equations introduced in [Toner & Tu (1998b)]. Here we introduced an additional term due to birth and death in the density equation.

We first find the mean field homogeneous ordered steady state of Eqs.(2.3) and (2.4), $\rho = \rho_0$ and $\mathbf{P} = P_0 = \sqrt{\frac{\alpha_1(\rho_0)}{\alpha_2}}\hat{\mathbf{x}}$. We further add small perturbation on the above homogeneous ordered state and write: $\rho(\mathbf{r},t) = \rho_0 + \delta\rho(\mathbf{r},t)$ and $\mathbf{P}(\mathbf{r},t) = (P_0 + \delta P_x)\hat{x} + \delta P_y \hat{y}$. The perturbations $\delta\rho(\mathbf{r},t)$, $\delta P_x(\mathbf{r},t)$ and $\delta P_y(\mathbf{r},t)$ are the small fluctuations in the density and two components of polarisation respectively. Since the system shows a mean-field transition from disordered-to-ordered state where α_1, changes sign. We assumed that system is close to the critical point such that order parameter is small and hence we have calculated the model for $\alpha_1 = 0$ (at the mean field critical point). The change in the critical point going beyond the mean field study in an another interesting research problem and explored in other previous studies of active systems [Das et al. (2017)]. We further substitute for the ρ and $\mathbf{P}$ from the above expressions and write the Eqs. (2.3) and (2.4) for the small fluctuations $\delta\rho, \delta P_x$ and δP_y to the linear order. The equation for δP_x, will not contribute to linear order. Hence only the equations for the local density fluctuation $\delta\rho(\mathbf{r},t)$ and local transverse polarisation fluctuation $\delta P_y(\mathbf{r},t)$ will survive.

$$\partial_t \delta\rho(r,t) = -v_0 \partial_y \delta P_y - \gamma\rho_0 \delta\rho + D_\rho \nabla^2 \delta\rho \tag{2.5}$$

$$\partial_t \delta P_y = -\partial_y \frac{v_1}{2\rho_0} \delta\rho + D\nabla^2 \delta P \tag{2.6}$$

We further take the Fourier transform of the two equations using

$$\hat{\mathbf{A}}(\mathbf{q},\omega) = \int \mathbf{A}(\mathbf{r},t)\exp(i\mathbf{q}\cdot\mathbf{r} + i\omega t)d\mathbf{r}dt;$$

where $\hat{\mathbf{A}} = (\delta\hat{\rho}, \delta\hat{P}_y)$. We use the method of Fourier transform to solve the modes of the coupled non-linear partial differential equations of motion for the density and polarisation in Eqs. (2.3) and (2.4). The similar approach is used earlier in the system of polar flock as well as in fluid mechanics in [Forster et al. (1977); Toner & Tu (1998b)]. Applying the Fourier transform, the two equations will become:

$$(-i\omega + D_\rho q^2 + \gamma\rho_0)\delta\rho + iq_y v_0 \rho_0 \delta P_y = 0 \tag{2.7}$$

and

$$iq_y \frac{v_1}{2\rho_0} \delta\rho + (-i\omega + Dq^2)\delta P_y = 0 \tag{2.8}$$

The fields $(\delta\rho, \delta P_y)$ in Eqs. (2.7) and (2.8) and later equations are in the Fourier transform but the $\hat{}$ symbol is removed for simplicity. The wavevector $\mathbf{q} = (qcos(\theta), qsin(\theta)) = (q_x, q_y)$, θ is the angle from the direction of broken symmetry.

We further solve the above two coupled linear equations for $\delta\rho$ and δP_y (2.7) and (2.8) respectively and find the solution for the two modes $\omega_\pm$ as;

$$\omega_\pm = \frac{-i\gamma\rho_0}{2} \pm \frac{q}{2}\sqrt{2v_0 v_1 + 2\gamma\rho_0(D_\rho - D)} \tag{2.9}$$

The first term in the two modes shows the exponential decay of the two fields (density and polarisation) due to the nonzero birth and death $\gamma \neq 0$, that represents the decay of traveling mode for finite birth and death. The second term is like sound mode, with speed proportional to the system parameters (self-propulsion speed of the particles and two diffusion constants).

In the next section we carry out the perturbative study of the hydrodynamic equations of motion to the lowest (quadratic) order nonlinearity. The aim of the perturbative study is to solve the coupled equations for the density and write an effective equation for the polarisation. The effective polarisation equation is renormalised and hence we name the method as renormalised mean field study.

2.4.1 Perturbative calculation for effective free energy for local polarisation

We focus our study near the disorder-to-ordered critical point and aim to write an effective renormalised equation for polarisation after solving for density. To do so, we assume the polarisation fluctuation is small and perform the study around the isotropic or disordered state as in usual Landau-Ginzburg approach [Chaikin et al. (1995)].

We introduce; $\rho = \rho_0 + \delta\rho$ and $\mathbf{P} = (\delta P_x, \delta P_y)$ and write the equations for the small fluctuations $\delta\rho$ and $\delta\mathbf{P} = (\delta P_x, \delta P_y)$. The solution for the Fourier transformed local density fluctuation $\delta\rho(\mathbf{q},\omega)$ and polarisation fluctuations $\delta\mathbf{P}(\mathbf{q},\omega)$ will become;

$$\begin{aligned}\delta\rho(\mathbf{q},\omega) = &\frac{-v_0\rho_0 i\mathbf{q}.\delta\mathbf{P}(\mathbf{q},\omega)}{(-i\omega + D_\rho q^2 + \gamma\rho_0)} \\ &-\frac{1}{2}\frac{v_0 i\mathbf{q}.\int[\delta P(\mathbf{k},\Omega)\delta\rho(\mathbf{q}-\mathbf{k},\omega-\Omega) + \delta P(\mathbf{q}-\mathbf{k},\omega-\Omega)\delta\rho(k,\omega)]d\mathbf{k}d\Omega}{(-i\omega + D_\rho q^2 + \gamma\rho_0)}\end{aligned} \tag{2.10}$$

and

$$\begin{aligned}-i\omega\delta\mathbf{P}(\mathbf{q},\omega) = \alpha_1(\rho_0)\delta\mathbf{P}(\mathbf{q},\omega) \\ &+\alpha_1{}'(\rho_0)\frac{1}{2}\left[\int\delta\mathbf{P}(\mathbf{k},\Omega)\delta\rho(\mathbf{q}-\mathbf{k},\omega-\Omega) + \delta\mathbf{P}(\mathbf{q}-\mathbf{k},\omega-\Omega)\delta\rho(\mathbf{k},\Omega)d\mathbf{k}d\Omega\right] \\ &-\alpha_2\int\delta\mathbf{P}(\mathbf{k},\Omega)\delta\mathbf{P}(\mathbf{k}',\Omega-\Omega')\delta\mathbf{P}(\mathbf{q}-\mathbf{k}-\mathbf{k}',\omega-\Omega-\Omega')d\mathbf{k}d\mathbf{k}'d\Omega d\Omega\end{aligned} \tag{2.11}$$

Here we write only first two terms in the polarisation Eq.((2.4)). $\alpha_1'(\rho_0) = \frac{\partial\alpha_1}{\partial\rho}\Big|_{\rho=\rho_0}$. Substitute for $\delta\rho$ leading order from Eq.(2.10) and substituting for one of mode ω_+ from Eq.(2.9)

$$
\begin{aligned}
-i\omega\delta\mathbf{P}(\mathbf{q},\omega) = \; & \alpha_1(\rho_0)\delta\mathbf{P}(\mathbf{q},\omega) + \frac{1}{2}\alpha_1{}'(\rho_0)\left[\frac{\int(\delta\mathbf{P}(\mathbf{k})(v_0\rho_0(\mathbf{q}-\mathbf{k}))\delta\mathbf{P}(\mathbf{q}-\mathbf{k},\omega-\Omega))}{6\gamma\rho_0+(q-k)\sqrt{2v_0v_1+\gamma\rho_0(D_\rho-D)}}\right. \\
& \left. + \frac{\int(\delta\mathbf{P}(\mathbf{q}-\mathbf{k},\omega-\Omega)(v_0\rho_0\mathbf{k})\delta\mathbf{P}(\mathbf{k},\Omega))}{\gamma\rho_0+k\sqrt{2v_0v_1+\gamma\rho_0(D_\rho-D)}}\right] \\
& \alpha_2\int\delta\mathbf{P}(\mathbf{k},\Omega)\delta\mathbf{P}(\mathbf{k}',\Omega-\Omega')\delta\mathbf{P}(\mathbf{q}-\mathbf{k}-\mathbf{k}',\omega-\Omega-\Omega')d\mathbf{k}d\mathbf{k}'d\Omega d\Omega
\end{aligned}
\tag{2.12}
$$

It is complicated to solve the above equation for the dimensions $d=2$, when $\delta\mathbf{P}$ is a vector. However the usual flocking transition is characterised by the appearance of bands near the transition [Bhattacherjee et al. (2015); Chaté et al. (2008); Solon & Tailleur (2013)]. When bands form, the local density and polarisation shows the variation only along the direction of moving bands and in the transverse direction it is homogeneous both in space and time. Hence system can be considered one dimensional where both $\delta\mathbf{P}$ and $\delta\rho$, only vary along the direction of moving bands and all the vectors can be replaced by scalars in Eq.(2.12). In such conditions, we can rewrite the above Eq.(2.12) as

$$
\begin{aligned}
-i\omega\delta P(\mathbf{q},\omega) = \; & \alpha_1(\rho_0)\delta P(q,\omega) \\
& + \frac{1}{2}\alpha_1'(\rho_0)\left[\frac{v_0\rho_0\int\delta P(q-k,\omega-\Omega)(q-k)\delta P(k,\Omega)dkd\Omega}{6\gamma\rho_0+(q-k)\sqrt{2v_0v_1+\gamma\rho_0(D_\rho-D)}}\right. \\
& \left. + \frac{v_0\rho_0\int\delta P(q-k,\omega-\Omega)k\delta P(k,\Omega)dkd\Omega}{6\gamma\rho_0+k\sqrt{2v_0v_1+\gamma\rho_0(D_\rho-D)}}\right] \\
& - \alpha_2\int\delta P(k,\Omega)\delta P(k',\Omega')\delta P(q-k-k',\omega-\Omega-\Omega')dkdk'd\Omega d\Omega'
\end{aligned}
\tag{2.13}
$$

Case with no birth and death :
For $\gamma=0$ or no birth and death, by doing the inverse Fourier transform, we write the effective free energy $\mathscr{F}_{eff}(\delta P)$ using Eq.(2.13) as

$$
\mathscr{F}_{eff}(\delta P) = -\frac{\alpha_1(\rho_0)}{2}\int d^2r(\delta P(r))^2 - \frac{\alpha_1'(\rho_0)}{6}\sqrt{\frac{v_0}{2v_1}}\int d^2r(\delta P(r))^3 + \alpha_2\frac{1}{4}\int d^2r(\delta P(r))^4
\tag{2.14}
$$

For homogeneous δP, the effective free energy $\mathscr{F}_{eff}(\delta P)$ is real space will become

$$
\mathscr{F}_{eff}(\delta P) = -\alpha_1(\rho_0)\frac{\delta P^2}{2} - \frac{\alpha_1'(\rho_0)}{6}\sqrt{\frac{v_0}{2v_1}}\delta P^3 + \frac{\alpha_2}{4}\delta P^4
\tag{2.15}
$$

The constants appearing in Eq.(2.15) due to finite volume integration are absorbed in the coefficients. The second term of the right hand side of Eq.(2.15) is an additional expression which is cubic in order $\mathscr{O}(\delta P^3)$. The presence of such nonlinear term can lead the mean-field transition to first order.

Case with birth and death:
Now we examine the system for finite γ, using the denominator of Eq.(2.13) inside the square [..] bracket

$$\gamma\rho_0 \gg \frac{q\sqrt{2v_0v_1+\gamma\rho_0(D_\rho-D)}}{6} \tag{2.16}$$

Then, the second term in Eq.(2.13) is of the form of $(P\nabla P)$ and this term can be compared with the convective nonlinear term of the type $\mathbf{P}\cdot\nabla\mathbf{P}$ in the hydrodynamic Eq.(2.4).

Hence for large γ, the birth and death term will dominate and the transition will be of the continuous type as predicted by mean field theory, whereas for finite and small γ such that

$$\gamma\rho_0 \ll \frac{q\sqrt{2v_0v_1+\gamma\rho_0(D_\rho-D)}}{6} \tag{2.17}$$

the effective free energy for $\mathscr{F}_{eff}(\delta P)$ will become

$$F_{eff}(\delta P) = -\frac{1}{2}\alpha_1(\rho_0)\delta P^2 - \frac{v_0\rho_0\alpha_1'(\rho_0)\delta P^3}{6\sqrt{2v_0v_1+\gamma\rho_0(D_\rho-D)}} + \frac{\alpha_2}{4}\delta P^4 \tag{2.18}$$

the wavevector dependence of additional convective non-linear term in Eq.(2.13) goes away and it contributes an additional $\mathscr{O}(\delta P^3)$ nonlinearity in the effective free energy which will lead the transition to discontinuous type. Therefore the discontinuous transition happens through the competition of a length scale and birth and death parameter as given in Eq. (2.17). As shown in Fig.[2.4], on increasing birth and death term from $\gamma = 0$, the bands start splitting and their size deceases, and the nature of transition becomes more and more continuous type as predicted by mean-field theory.

We further analysed the properties of effective free energy in the presence of additional cubic order nonlinearity. In simplified notation the effective free energy in Eq.(2.18) can be rewritten as

$$\mathscr{F}(\delta P) = -\beta_1\delta P^2 - \beta_2\delta P^3 + \beta_3\delta P^4 \tag{2.19}$$

where $\beta_1 = \frac{1}{2}\alpha_1(\rho_0)$, $\beta_2 = \frac{v_0\rho_0\alpha_1'(\rho_0)}{6\sqrt{2v_0v_1+\gamma\rho_0(D_\rho-D)}}$, $\beta_3 = \frac{\alpha_2}{4}$. For the transition to be first order we impose the coexistence condition i.e. $\mathscr{F}(\delta P = 0) = \mathscr{F}(\delta P \neq 0)$, that gives

$$-\beta_1 - \beta_2\delta P + \beta_3\delta P^2 = 0 \tag{2.20}$$

also the condition of steady state implies $\frac{\partial \mathscr{F}}{\partial \delta P} = 0$

$$-2\beta_1 - 3\beta_2\delta P + 4\beta_3\delta P^2 = 0 \tag{2.21}$$

using Eq.(2.20) and (2.21) the jump in the order parameter P at the transition

$$\delta P = \frac{\beta_2}{2\beta_3} \tag{2.22}$$

is always positive, hence the finite jump. Substituting the value of δP in Eq.(2.20) and solve for β_1, we $\beta_1 - \frac{\beta_2^2}{4\beta_3} = 0$. We rewrite the above expression and get $\beta_1^c = \frac{\beta_2^2}{4\beta_3}$ again a positive term. We further analyse the jump in the order parameter and transition point by substituting the value β_2 and β_3 in Eq.(2.22), we get $\delta P = \frac{4v_0\rho_0\alpha_1'(\rho_0)}{3\alpha_2\sqrt{2v_0v_1+\gamma\rho_0\triangle D}}$ where $\triangle D = D_\rho - D$.

Assuming the temperature dependence of α_1 in the mean-field theory $\alpha_1(\rho,T) = \alpha_0(\rho)(T-T^*)$, T^* is point where there is a mean-field type second order phase transition for large γ. Here, if we define the true critical temperature as T_c, where $\beta_1 = \frac{\beta_2^2}{4\beta_3}$, we get the critical point $\alpha_1^c(\rho,T) = \alpha_0(\rho)(T_c - T^*) = 2\beta_1 > 0$. Hence we find that $T_c > T^*$ and $T_c = \frac{\beta_2^2}{2\beta_3\alpha_0} + T^*$. After substituting the value of β_2 and β_3, we find $T_c = T^* + \frac{2{v_0}^2{\rho_0}^2{\alpha_0'}^2\rho_0}{9(2v_0v_1+\gamma\rho_0\triangle D)\alpha_2\alpha_0(\rho_0)}$. Hence in the simplified notation we can write

$$T_c = T^* + \frac{A}{B+\gamma} \tag{2.23}$$

where $A = \frac{4{v_0}^2{\rho_0}^2{\alpha_0'}^2\rho_0}{9\rho_0\Delta D\alpha_2\alpha_0(\rho_0)}$ and $B = \frac{2v_0v_1}{\rho_0\Delta D}$. For large γ, second term in the expression for T_c is negligible and critical point happens at T^*. As we start tuning γ towards lower values, the phase transition shift towards right as obtained in our numerical study shown in Fig.[2.3]. Also δP (the jump in order parameter) is almost zero for large γ that means system approaches critical point continuously as found in our numerical study Fig.[2.6](b). But as we start decreasing γ transition happens with a finite jump in order parameter Fig.[2.6](a).

2.5 Conclusion

We studied a system of active Ising spins with birth and death on a two dimensional substrate with periodic boundary condition. The system is studied using Metropolis Monte Carlo method for the interaction among the spins and the spin perform the biased move along their direction of orientation. System is studied for fixed activity and varying birth and death rate γ. Its shows a phase transition from disorder-to-order for all γ and fixed activity on varying temperature from high to low. The transition is of first order or discontinuous type for conserved model ($\gamma = 0$) and becomes second order continuous type for the birth and death model. Also transition shifts towards higher temperature on decreasing γ. Hence the presence of birth and death term tune the disorder-to-order transition to lower temperature and shows a crossover from discontinuous to continuous type in the polar flock.
We also performed and compared the hydrodynamic approach developed for the continuum model with the numerical study performed for the lattice system. The results are compared for the local density and polarisation, which can be assumed like continuum in the steady state. In our analytical study we find that for zero birth and death rate, the phase transition is of first order with a finite jump in the polarisation as given in Eq.(2.22), whereas as we increase γ, the jump decreases. Hence we find a crossover from discontinuous type of transition to continuous type on increasing γ. Also the critical temperature shifts towards higher values as birth and death rate γ decreases in Eq.(2.23) and matches with what is observed in the numerical simulation Fig.[2.3]. Hence our study shows effect of birth and death on the nature of phase transition of polar-flock. The present model is studied for discrete Ising spins with the Globular conserved model [Binder et al. (2000)] for the spin interaction. It is worth to study the system for the non-conserved models like proliferating/decaying active matter and Kawasaki type [Binder (1987)] of spin interaction as well for the off lattice systems.

****